Electronic Supplementary Material (ESI) for Inorganic Chemistry Frontiers.

Supporting Information

Understanding the Synergistic Influence of Propylammonium Bromide Additive and Erbium Doped $CsPbI_2Br$ for Highly Stable Inorganic Perovskite Solar Cells

Jyoti V. Patil,[a, b] Sawanta S. Mali,[b] Shivaji B. Sadale,[c] Chang Kook Hong [a, b*]

[a]Optoelectronic Convergence Research Center, School of Chemical Engineering, Chonnam National University, Gwangju, South Korea 61186.

[b]Polymer Energy Materials Laboratory, School of Chemical Engineering, Chonnam National University, Gwangju, South Korea 61186.

[c]Department of Technology, Shivaji University, Kolhapur, 416004, Maharashtra, India

***Corresponding author**: hongck@chonnam.ac.kr

S1: Details of different chemicals:

The chemical materials including cesium iodide (CsI) (Sigma, 99.999 %), lead bromide ($PbBr_2$) (Sigma, ≥ 98%), lead iodide (PbI_2) (Sigma, 99%), erbium (III) chloride ($ErCl_3$) (Sigma, 99.99%), *n*-Propylammonium bromide (PABr) (Sigma, 99.99%), dimethyl sulfoxide (DMSO), (N, N-dimethylformamide (DMF), poly(3- hexylthiophene-2,5-diyl) (P3HT) (Sigma-Aldrich, average Mw 50,000-100,000) were purchased from Sigma-Aldrich. The hot-air gun (BOSCH, GHG 630 DCE Hot Air Gun -0601 94C 740) was used as a hot-air source.

S2: Details of different characterization of perovskite material and IPVSC-based devices:

The surface morphological images were recorded by a scanning electron microscope (SEM; S-4700, Hitachi). The X-ray diffraction (XRD) measurements were carried out using a D/MAX Ultima III-XRD spectrometer (PAN analysis, Japan) with Cu Kα line of 1.5410 Å. Optical absorption measurements were carried out on a UV-vis spectrophotometer (Varian, CARY, 300 Conc.) in the 500-900 nm wavelength range. Energy-dispersive X-ray (EDX) elemental mapping was carried out in the scanning transmission electron microscopy (STEM) mode. The contrast against the background of HAADF-STEM image has been carried out background selection: Rois mode at detector angle: 14.6 degree. The elemental information was studied using an X-ray photoelectron spectroscopy (XPS) (VG Multilab 2000-Thermo Scientific, USA, K-Alpha) with a multi-channel detector, which can endure high photonic energies from 0.1 to 3 keV. The ultraviolet-photoelectron spectroscopy (UPS) measurements were carried out using Thermo VG Scientific Sigma Probe, UK, UV Monochromatic He I (21.22 eV) gas, (Bias -5.0 V, Aperture size 8 mm adjustable) for UPS base UHV pressure 1 x 10^{-9} mB without surface treatment. The spectral response was taken by a spectral IPCE measurements system (K3100, Mc-Science), which was equipped with a monochromator, a K240×E 300 lamp source connected with K401 OLS XE300W lamp power supply and a K102 signal amplifier. Prior to the use of the light intensity were calibrated using a Si-photodiode (Model: S1337-1010BQ) and In GaAs photodiode (model: G12180-050A) for 300-1100 nm and 1100-1400 nm calibration respectively. Measurements were taken in EQE mode. Time-resolved photoluminescence (TRPL) decay transients were measured at 650 nm using excitation with a 470 nm light pulse at a frequency of 5MHz from the Spectrophotometer F-7000.

The IPVSCs were illuminated using a solar simulator at AM 1.5 G for 10 s, where the light intensity was adjusted with an NREL-calibrated Si solar cell with a KG-5 filter to 1 sun intensity

(100 mW cm^{-2}). The photovoltaic performance of IPVSC devices were measured by metal shadow masks with active small area of 0.3 x 0.3 =0.09 cm^2. The exact illumination to the active area was fixed via attaching thin metal shadow mask from back side throughout measurements. The *J-V* curves were measured along with the reverse scan direction from 1.5 V to − 0.05 V or the forward scan direction from −0.05 V to 1.5 V. Using the Mott–Gurney law, the trap density of the electron-only device with an architecture of FTO/mp-TiO_2/perovskite/PCBM/Ag was measured with the space charge limited current (SCLC) model from 0 to 7 V under dark conditions. The Nyquist plots were obtained via conducting electrochemical impedance spectroscopy (EIS) analysis with the help of Iviumstat (Ivium Technologies B.V., Eindhoven, and the Netherlands) at an open-circuit potential at frequencies ranging from 10^{-1} to 10^5 Hz with AC amplitude of 10 mV. For equivalent circuit analysis, Z-view 2.8d was used. The steady-state efficiencies were obtained by tracking the maximum power point. The IPVSC devices were illuminated using a solar simulator at AM 1.5 G for 10 s, where the light intensity was adjusted with an NREL-calibrated Si solar cell with a KG-5 filter to 1 sun intensity (100 mW cm^{-2}). The device stability was tested in an air at 65 °C without encapsulation and after measurement devices were stored in ambient conditions. The *J-V* curves were periodically measured under AM1.5 G simulated sunlight at room temperature. For thermal stability, perovskite devices were kept on the hot plate at 65 °C and taken out during measurements. We monitored devices temperature ~ 20 °C by continuous air-steam flow and relative humidity was ~ 30 % for continuous illumination testing.

Figure S1: (a) The Cs, CsEr and CsEr-PA perovskite thin films deposited by the hot air flow method and (b) time dependent photographs of the Cs, CsEr and CsEr-PA-based perovskite thin films.

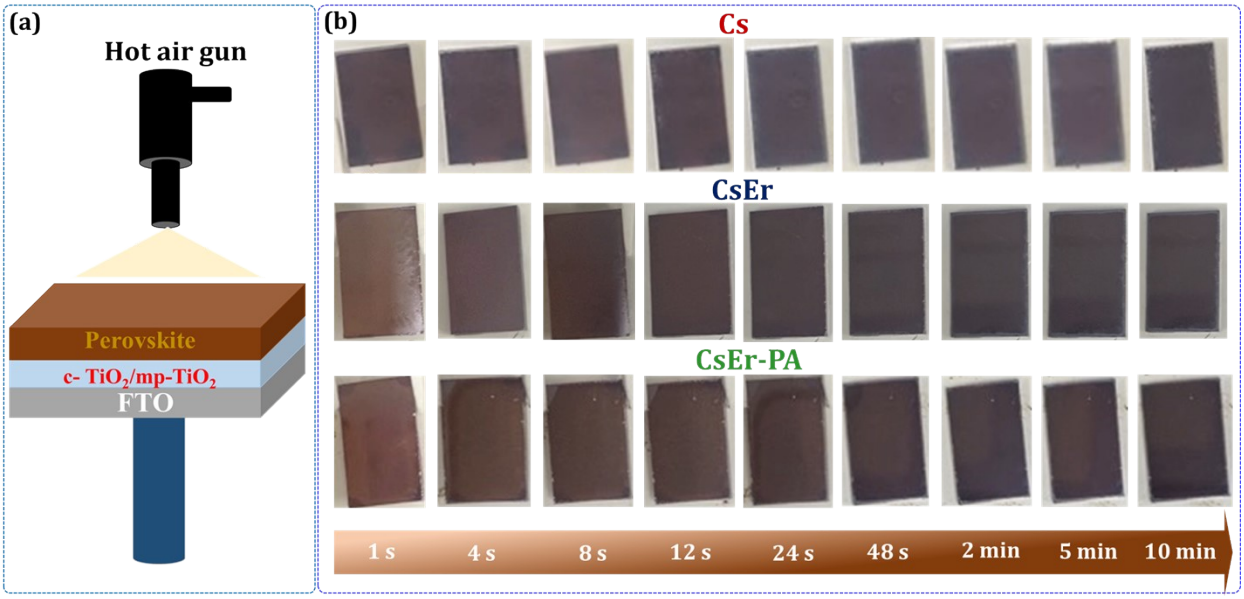

Figure S2: SEM images: (a) $CsPbI_2Br$, (b) Cs-1 mg ml^{-1} PABr, (c) Cs-2 mg ml^{-1} PABr, (d) Cs-3 mg ml^{-1} PABr and (e) Cross section of Cs-2 mg ml^{-1} PABr-based IPVSC.

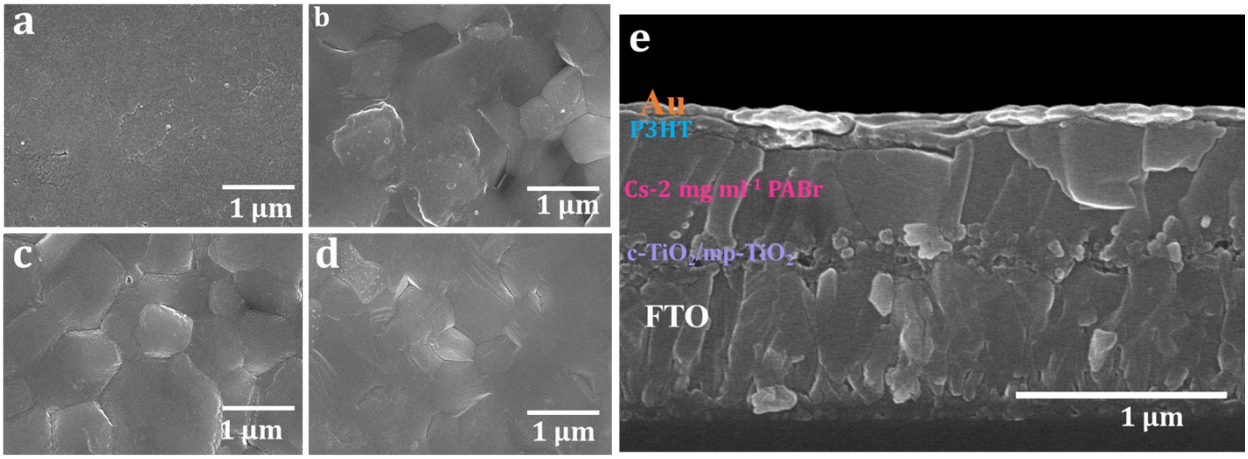

Figure S3: Scanning electron microscopic images: (a) $CsPb_{0.99}Er_{0.01}I_2BrCl_{0.03}$, (b) $CsPb_{0.98}Er_{0.02}I_2BrCl_{0.06}$, (d) $CsPb_{0.97}Er_{0.03}I_2BrCl_{0.09}$, (d) $CsPb_{0.96}Er_{0.04}I_2BrCl_{0.12}$ perovskite films.

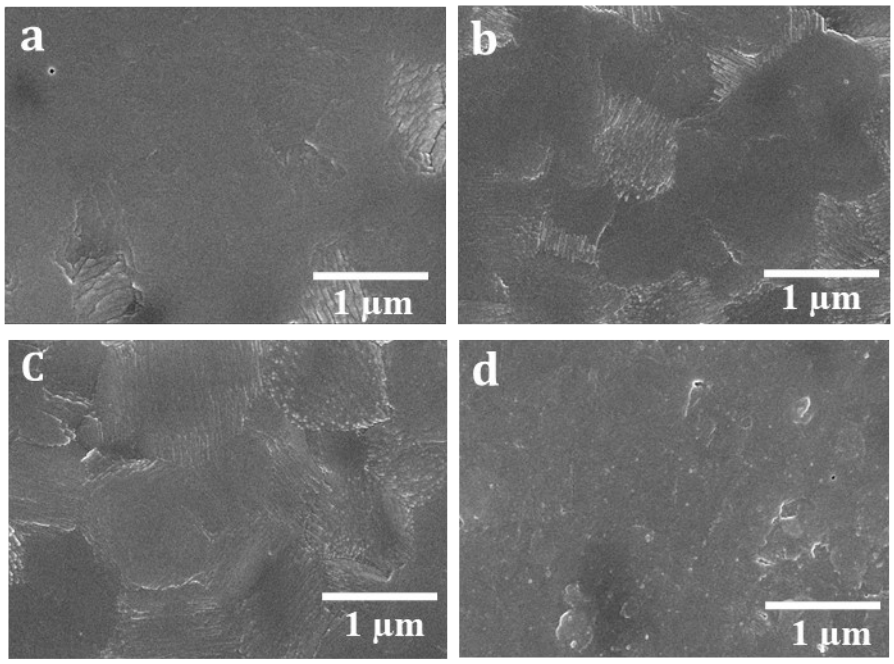

Figure S4: **Scanning electron microscopic images:** (a) CsEr-1mg ml^{-1} PABr, (b) CsEr-2mg ml^{-1} PABr, (c) CsEr-3mg ml^{-1} PABr and (d) CsEr-4mg ml^{-1} PABr-based perovskite thin films.

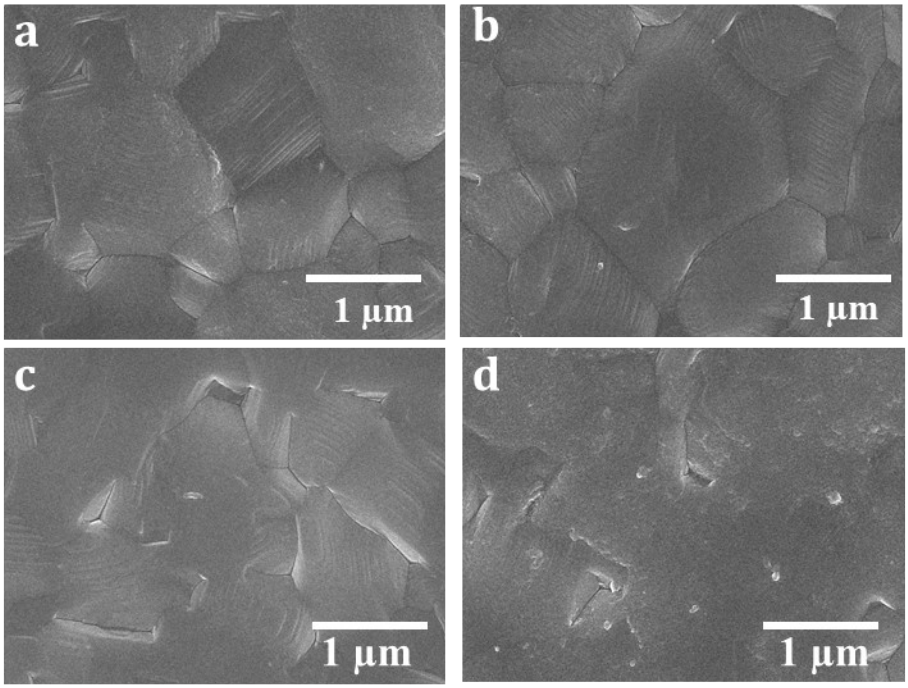

Figure S5: Elemental mapping: (a) HAADF STEM image, (b) cesium, (c) lead, (d) iodide, (e) bromide, (f) erbium and (g) chloride.

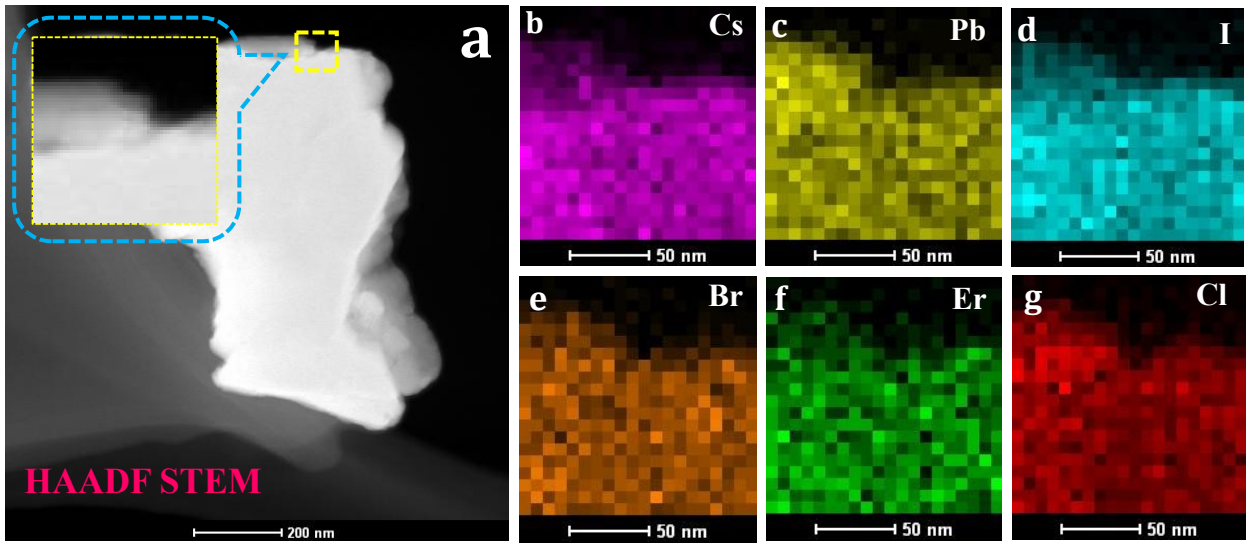

Figure S6: (a) Cross-sectional SEM image and (b) elemental mapping of $ErCl_3$ doped $CsPbI_2Br$-based perovskite layer.

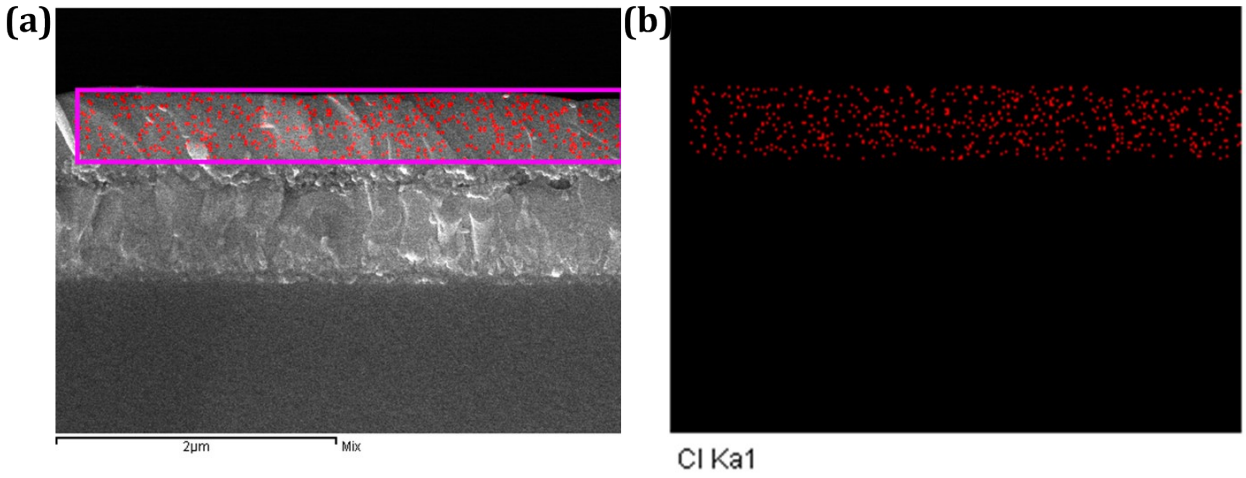

Figure S7: Magnified X-ray diffraction (XRD) patterns (2θ=12-18) of Cs, CsEr and CsEr-PA perovskite films.

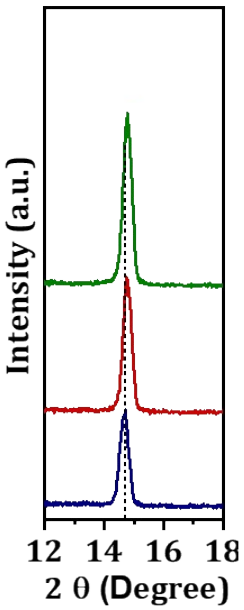

Figure S8: Tauc plots of the Cs, CsEr and CsEr-PA perovskite thin films calculated from the UV-Vis absorption spectra.

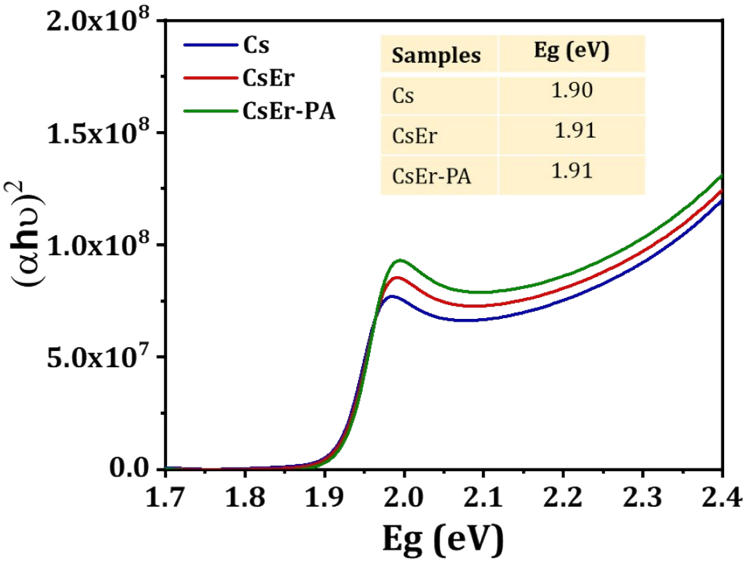

Figure S9: (a) UPS survey spectra of perovskite films, valence band region of the (b) Cs, (c) CsEr and (d) CsE-PA perovskites on the mp-TiO_2/FTO substrate.

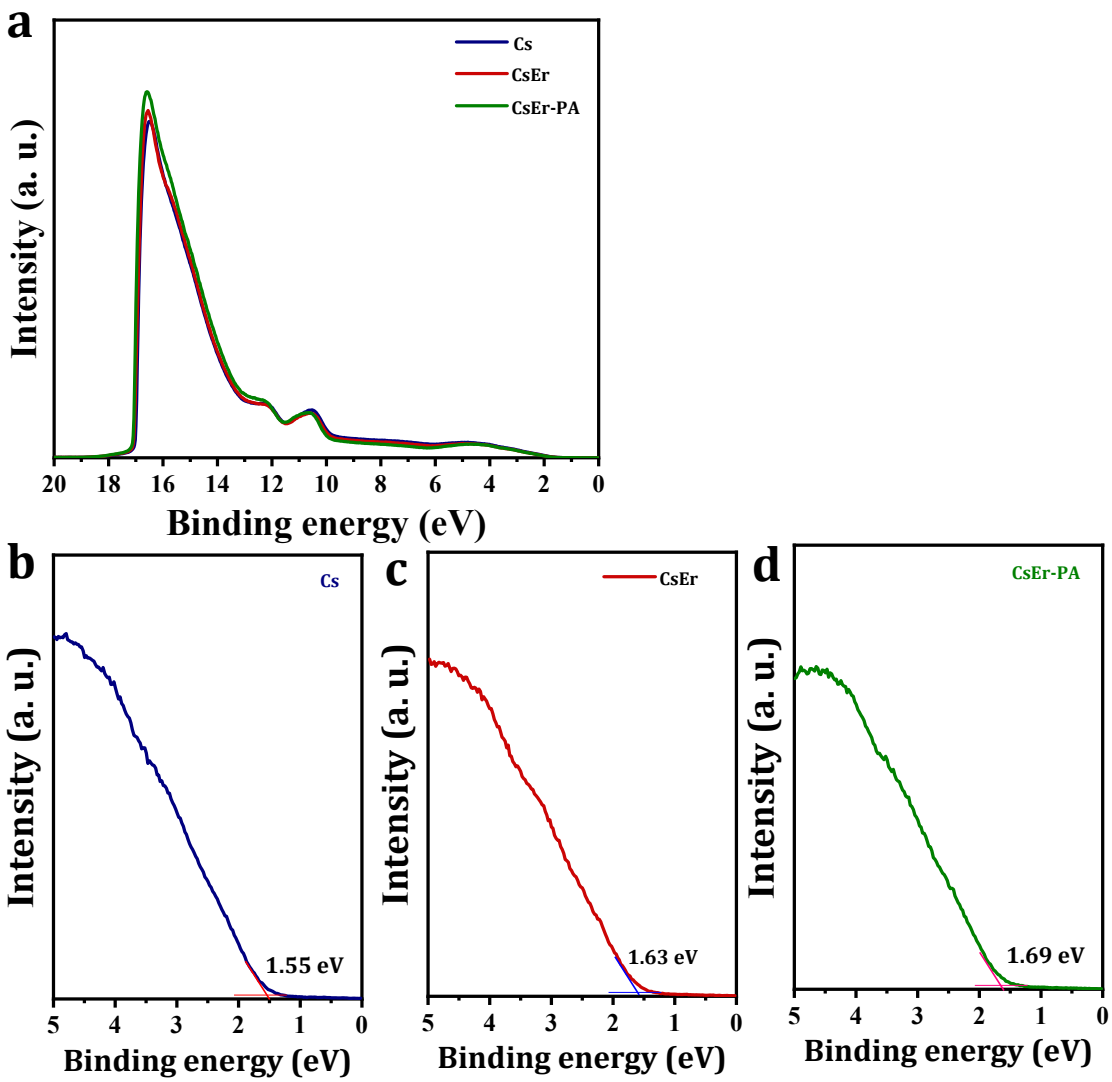

Figure S10: *J-V* curve of the different amounts of the PABr (1 - 3 mg ml^{-1}) additive added $CsPbI_2Br$ perovskites-based IPVSC devices.

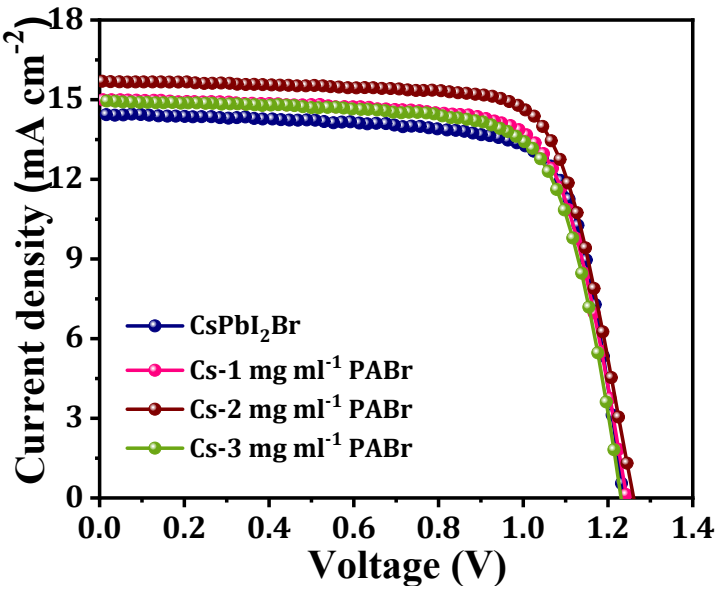

Figure S11: *J-V* curves of the $CsPb_{0.99}Er_{0.01}I_2BrCl_{0.03}$, $CsPb_{0.98}Er_{0.02}I_2BrCl_{0.06}$, $CsPb_{0.97}Er_{0.03}I_2BrCl_{0.09}$, $CsPb_{0.96}Er_{0.04}I_2BrCl_{0.12}$ perovskites-based IPVSC devices.

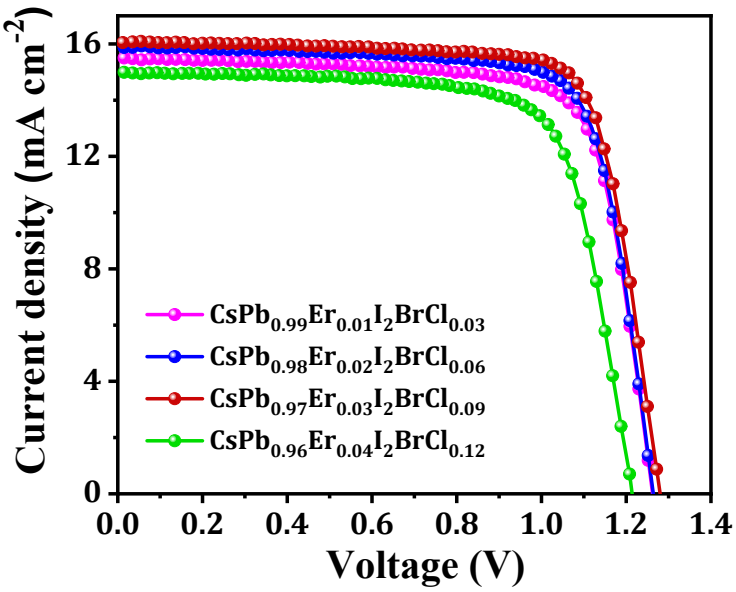

Figure S12: *J-V* curves of the CsEr-1 mg ml^{-1} PABr, CsEr-2 mg ml^{-1} PABr, CsEr-3 mg ml^{-1} PABr and CsEr-4 mg ml^{-1} PABr perovskites-based IPVSC devices.

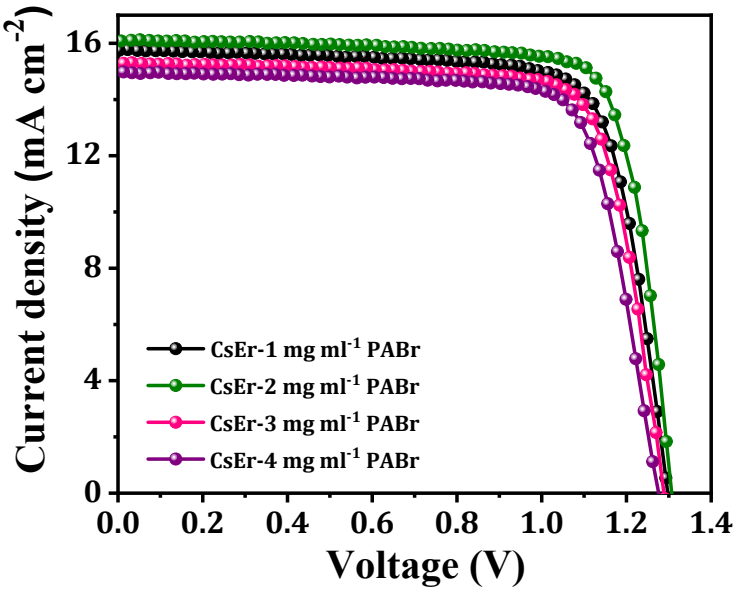

Table S1: XPS core-level peak positions of the Cs, CsEr and CsEr-PA-based perovskite thin films.

	$CsPbI_2Br$			**CsEr**			**CsEr-PA**		
Core level	Start BE	Peak BE	End BE	Start BE	Peak BE	End BE	Start BE	Peak BE	End BE
Cs3d5	728.03	**724.46**	719.97	731.23	**724.56**	719.31	728.45	**724.64**	720.24
Cs3d3	741.89	**738.41**	734.89	744.01	**738.5**	732.94	742.32	**738.61**	735.33
Pb4f7	139.99	**137.81**	134.39	139.99	**137.81**	134.39	140.64	**138.06**	134.45
Pb4f5	147.24	**142.8**	139.99	147.24	**142.8**	139.99	147.45	**143.04**	140.64
I3d5	623.2	**618.88**	613.58	623.07	**618.95**	613.99	624.52	**619.05**	613.64
I3d3	633.95	**630.35**	625.8	634.55	**630.42**	626.06	635.16	**630.53**	626.03
Br3d	71.16	**68.03**	63.8	71.57	**68.35**	64.77	71.43	**68.37**	64.81
Er3d	-	**-**	-	174.19	**169.45**	167.15	174.93	**169.86**	166.76

Table S2: Different parameters calculated from the XRD of the Cs, CsEr and CsEr-PA-based perovskite thin films.

Perovskites	Main peak position (°)	FWHM (main peak)	$d_{(100)}$ spacing (nm)	Lattice constant (nm)
Cs	14.63	0.180	0.6049	0.6048
CsEr	14.66	0.324	0.6034	0.6033
CsEr-PA	14.67	0.330	0.6032	0.6031

Table S3: TRPL measurements of the Cs, CsEr and CsEr-PA-based perovskite thin films deposited on the mp-TiO_2/FTO substrates.

Perovskites films	τ_1 (ns)	τ_2 (ns)	τ_3 (ns)	A_1*	A_2*	A_3*	$\langle\tau_{avg}\rangle$ (ns)
Cs	17	3.2	0.901	6.5	3.4	0.98	4.19
CsEr	41	7.6	1.6	7.5	2.3	0.149	11
CsEr-PA	103	11	2	5.7	3.6	0.1266	30

Table S4: Calculated parameters for energy level of the Cs, CsEr and CsEr-PA-based perovskite films from UPS spectra.

Perovskites	E_{cutoff} (eV)	WF (eV)	E_{onset} (eV)	VBM (eV)	ΔEg (eV)	CBM (eV)
Cs	17.03	4.19	1.30	5.49	1.90	3.59
CsEr	17.07	4.15	1.31	5.46	1.91	3.55
CsEr-PA	17.11	4.11	1.33	5.44	1.91	3.53

***WF** = 21.22-Ecutoff, **VBM** = WF + Eonset, **CBM** = VBM-Eg*

Table S5: *J-V* analysis of the $CsPbI_2Br$, Cs-1 mg ml^{-1} PABr, Cs-2 mg ml^{-1} PABr and Cs-3 mg ml^{-1} PABr perovskites-based IPVSC devices.

Perovskites	V_{OC} (V)	J_{SC} (mA cm^{-2})	FF (%)	PCE (%)
$CsPbI_2Br$	1.235	14.45	74.18	13.20
Cs-1 mg ml^{-1} PABr	1.241	15.08	74.24	13.89
Cs-2 mg ml^{-1} PABr	1.261	15.69	74.42	14.72
Cs-3 mg ml^{-1} PABr	1.228	14.97	73.49	13.50

Table S6: *J-V* analysis of the $CsPb_{0.99}Er_{0.01}I_2BrCl_{0.03}$, $CsPb_{0.98}Er_{0.02}I_2BrCl_{0.06}$, $CsPb_{0.97}Er_{0.03}I_2BrCl_{0.09}$ and $CsPb_{0.96}Er_{0.04}I_2BrCl_{0.12}$ perovskites-based IPVSC devices.

Perovskites	V_{OC} (V)	J_{SC} (mA cm^{-2})	FF (%)	PCE (%)
$CsPb_{0.99}Er_{0.01}I_2BrCl_{0.03}$	1.260	15.49	75.58	14.75
$CsPb_{0.98}Er_{0.02}I_2BrCl_{0.06}$	1.262	15.89	76.00	15.24
$CsPb_{0.97}Er_{0.03}I_2BrCl_{0.09}$	1.280	16.01	76.79	15.73
$CsPb_{0.96}Er_{0.04}I_2BrCl_{0.12}$	1.212	15.00	72	13.08

Table S7: *J-V* analysis of the CsEr-1 mg ml^{-1} PABr, CsEr-2 mg ml^{-1} PABr, CsEr-3 mg ml^{-1} PABr and CsEr-4 mg ml^{-1} PABr perovskites-based IPVSC devices.

Perovskites	V_{OC} (V)	J_{SC} (mA cm^{-2})	FF (%)	PCE (%)
CsEr-1 mg ml^{-1} PABr	1.293	15.89	76.89	15.79
CsEr-2 mg ml^{-1} PABr	1.304	16.16	79.44	16.74
CsEr-3 mg ml^{-1} PABr	1.284	15.29	75.52	14.82
CsEr-4 mg ml^{-1} PABr	1.274	14.96	74.65	14.22

Table S8: EIS fitting parameters of the Cs, CsEr and CsEr-PA-based IPVSC devices.

Perovskites	R_S (Ω)	R_{rec} (Ω)
Cs	184.67	5337
CsEr	84.99	6544
CsEr-PA	45.59	7857

Table S9: Photovoltaic parameters of the Cs, CsEr and CsEr-PA-based IPVSCs.

	$CsPbI_2Br$				**CsEr**				**CsEr-PA**			
Sr. no	J_{SC} ($mAcm^{-2}$)	V_{OC} (V)	FF (%)	**PCE (%)**	Jsc ($mAcm^{-2}$)	V_{OC} (V)	FF (%)	**PCE (%)**	Jsc ($mAcm^{-2}$)	V_{OC} (V)	FF (%)	**PCE (%)**
1	1.105	12.10	67.50	**9.02**	1.160	14.55	72.89	**12.30**	1.198	14.77	76	**13.44**
2	1.130	12.86	68	**9.88**	1.163	14.58	72.95	**12.36**	1.205	14.88	76.35	**13.68**
3	1.135	12.95	68.52	**10.07**	1.166	14.60	73	**12.42**	1.210	14.93	76.42	**13.80**
4	1.143	13.0	68.85	**10.23**	1.176	14.70	73.25	**12.69**	1.215	15.05	76.58	**14**
5	1.154	13.10	68.91	**10.41**	1.188	14.85	73.76	**13.01**	1.219	15.10	76.70	**14.11**
6	1.161	13.29	69	**10.64**	1.198	15	74	**13.29**	1.230	15.25	76.86	**14.41**
7	1.172	13.48	69.35	**10.95**	1.200	15.02	74.45	**13.41**	1.245	15.35	77	**14.71**
8	1.185	13.95	69.49	**11.44**	1.210	15.15	75	**13.74**	1.253	15.40	77.35	**14.92**
9	1.191	14.00	70	**11.67**	1.221	15.23	75.88	**14.11**	1.265	15.45	77.40	**15.12**
10	1.199	14.05	70.85	**11.93**	1.237	15.52	76.22	**14.63**	1.277	15.56	77.56	**15.41**
11	1.209	14.09	71.20	**12.12**	1.245	15.66	76.41	**14.89**	1.284	15.71	78	**15.83**
12	1.222	14.15	72	**12.44**	1.258	15.75	76.72	**15.35**	1.286	15.88	78.45	**16.02**
13	1.228	14.36	73	**12.87**	1.268	15.81	76.84	**15.20**	1.292	16	78.56	**16.23**
14	1.231	14.41	74	**13.12**	1.276	15.95	76.69	**15.60**	1.300	16.10	78.71	**16.47**
15	1.235	14.45	74.18	**13.2**	1.280	16.01	76.79	**15.73**	1.304	16.16	79.44	**16.74**

❖ **TRPL measurement details**

The obtained TRPL lifetime parameters were well fitted with a tri-exponential decay function from equation S1 [S1].

$$I(t) = I_0 + A_1 \exp\left(-\frac{t-t_0}{\tau_1}\right) + A_2 \exp\left(\frac{-t-t_0}{\tau_2}\right) + A_3 \exp\left(\frac{-t-t_0}{\tau_3}\right) \quad --(S1)$$

Where, τ_1, τ_2 and τ_3 are first, second and third-order decay time, A_1, A_2 and A_3 are respective weight factors of each decay channel. Here, τ_1 stands for the fast decay lifetime and τ_2 and τ_3 stand for the slow decay function. The average lifetimes $<\tau_{avg}>$ of Cs, CsEr and CsEr-PA inorganic perovskite thin films were calculated from equation S2 [S1].

$$< \tau_{avg} >= \sum_n \frac{\Sigma A_n \tau_n^2}{\Sigma_m A_m \tau_m^2} \quad --(S2)$$

❖ **V_{OC} as a function of illumination intensity**

The ideality factor (η) yielded by the slope of the fitted data, which was calculated by equations S3 and S4 [S2].

$$V_{OC} = nkT \ln(I)/q + A \quad \text{-------} \ (S3)$$

Where, k = Boltzmann constant, T = the temperature in Kelvin, q = the elementary charge and A is a constant according to the Shockley−Read−Hall (SRH) recombination mechanism [S3]. Equation S3 can be simplified for η as,

$$\eta = \text{slope} \times \frac{q}{kT} \quad \text{-------} \ (S4)$$

❖ **Charge Transport Studies (Trap density)**

The trap density (N_t) of the Cs, CsEr and CsEr-PA perovskite devices can be calculated according to equation S5 via trap-filled limit voltage (V_{TFL}) [S4, S5].

$$N_t = \frac{2\varepsilon_0 \varepsilon V_{TFL}}{eL^2} \quad \text{------} \ (S5)$$

(Where ε_0 = permittivity of vacuum, ε = relative dielectric constant, e = elementary charge, and L= perovskite film thickness).

References:

[S1] S. S. Mali, J. V. Patil, H. J. Kim and C. K. Hong, Gallium cationic incorporated compact TiO_2 as an efficient electron-transporting layer for stable perovskite solar cells*, Matter,* 2019, **1**, 464.

[S2] C. G. Shuttle, B. O. Regan, A. M. Ballantyne, J. Nelson, D. D. Bradley and J. R. Durrant, Bimolecular recombination losses in polythiophene: fullerene solar cells, *Phys. Rev. B: Condens. Matter Mater. Phys.* 2008*,* **78**, 113201.

[S3] H. Wang, J. H. Hsu, G. Yang, C. Yu, Novel organic schottky barrier diode created in a single planar polymer film, *Adv. Mater.* 2016, **28***,* 9545–9549.

[S4] H. Y. Park, D. C. Lim, K. D. Kim and S. Y. Jang, Performance optimization of low-temperature-annealed solution-processable ZnO buffer layers for inverted polymer solar cells, *J. Mater. Chem. A* 2013, **1***,* 6327– 6334.

[S5] J. Zhu, B. He, Z. Gong, Y. Ding, W. Zhang, X. Li, Z. Zong, H. Chen and Q. Tang, Grain enlargement and defect passivation with melamine additives for high efficiency and stable $CsPbBr_3$ perovskite solar cells, *ChemSusChem,* 2020*,* **13**, 1834–1843.